



## Modelling of industrial-scale bioreactors using the particle lifeline approach

Gisela Nadal-Rey<sup>a,b</sup>, John M. Kavanagh<sup>c</sup>, Benny Cassells<sup>b</sup>, Sjef Cornelissen<sup>b,1</sup>,  
David F. Fletcher<sup>c</sup>, Krist V. Germaey<sup>a</sup>, Dale D. McClure<sup>d,\*</sup>

<sup>a</sup> Process and Systems Engineering Center (PROSYS), Department of Chemical and Biochemical Engineering, Technical University of Denmark, Building 228A, 2800 Kgs. Lyngby, Denmark

<sup>b</sup> Novozymes A/S, Fermentation Pilot Plant, Krogshøjvej 36, 2880 Bagsvaerd, Denmark

<sup>c</sup> The University of Sydney, School of Chemical and Biomolecular Engineering, Building J01, Camperdown, NSW 2006, Australia

<sup>d</sup> Department of Chemical Engineering, College of Engineering, Design and Physical Sciences, Brunel University, London, Uxbridge UB8 3PH, United Kingdom

### ARTICLE INFO

#### Keywords:

CFD Modelling  
Kinetics  
Large-scale bioreactor  
Mixing  
Particle lifelines

### ABSTRACT

A key factor in improving the performance of large-scale bioreactors is understanding the conditions experienced by the cells inside the reactor. This can be challenging due to the practical difficulties involved, hence there is increasing use of simulation to quantify the environmental conditions found in large-scale bioreactors. In this work we have used the particle lifeline approach to quantify the effect of the reactor design on the conditions experienced by two very commonly used industrial organisms (*Escherichia coli* and *Saccharomyces cerevisiae*). It was found that the cells in the stirred tank reactor tended to experience longer fluctuations of both starvation and overflow metabolism when compared with those in the bubble column, this behaviour being caused by differences in mixing between the two reactor designs. It was found that a significant (60%) fraction of the population in the stirred tank reactors experienced starvation conditions for a large fraction (>70%) of the time, with exposure to such conditions being likely to affect the cellular metabolism. Results from this work provide a detailed insight into the conditions experienced inside industrial-scale bioreactors operated at realistic conditions. Such data can be leveraged to optimise large-scale reactor designs as well as for the development of scale-down systems.

### 1. Introduction

Understanding the performance of industrial scale bioreactors is a topic of considerable importance, particularly given the increasing interest in and need for sustainable production technologies [1–4]. From an industrial perspective the aim is to minimize the cost of production. This can be done by ensuring the process is reliable and reproducible, ensuring efficient conversion of substrate to product (i.e., maximizing the yield), minimizing downstream processing costs (this can be done by maximizing the product concentration) and ensuring efficient equipment utilization (i.e., maximizing the productivity of the system) [5]. The performance of large-scale reactors is determined by the hydrodynamics of the system (as this governs mixing and mass transfer), the operating conditions (e.g., feed rates, stirrer speeds and superficial gas velocities), as well as the characteristics of the microorganism used [1, 6–8]. Understanding the behavior of industrial scale reactors is challenging due to the need to accurately model both the hydrodynamics of

the system as well as the growth and uptake kinetics of the microorganism.

Large-scale bioreactors are typically either bubble columns or stirred tanks, with the reactor design having an obvious influence on the hydrodynamics. Due to the challenges involved with performing experimental work at the industrial-scale, Computational Fluid Dynamics (CFD) has been increasingly [2,9–13] used as a tool to model large-scale bioreactors. Such models have the advantage of offering a high degree of spatial and temporal resolution. However, they have the disadvantage in that it is not possible to simulate the entirety of an industrial fermentation due to the computational demand involved. For this reason, CFD models are typically used to model ‘snapshots’ of a fermentation, with each snapshot typically being up to several minutes in length [9,14,15]. A consequence of this approach is that the biomass concentration is assumed to be fixed in such a CFD model, as the timescale for growth is less than the simulation time. The performance of the system can then be quantified by calculating the relevant process metrics using instantaneous results, and/or transient averages over the duration of the

\* Corresponding author.

E-mail address: [dale.mcclure@brunel.ac.uk](mailto:dale.mcclure@brunel.ac.uk) (D.D. McClure).

<sup>1</sup> Present address: DSM Food and Beverage, Center for Food Innovation, Alexander Fleminglaan 1, 2613 AX Delft, Netherlands

**Nomenclature**

$BP$	By-product concentration [ $\text{kg m}^{-3}$ ].	$q_O$	Specific oxygen uptake rate [ $\text{kg kg}^{-1} \text{h}^{-1}$ ].
$F_O$	Fraction of time spent by a particle in overflow conditions [-].	$t_s$	Time step size [s].
$F_S$	Fraction of time spent by a particle in starvation conditions [-].	$X$	Biomass concentration [ $\text{kg m}^{-3}$ ].
$G$	Glucose concentration [ $\text{kg m}^{-3}$ ].	$Y_{XBP}^{Of}$	Yield coefficient of biomass on by-product under overflow conditions [ $\text{kg kg}^{-1}$ ].
$\bar{G}$	Time-averaged glucose concentration [ $\text{kg m}^{-3}$ ].	$Y_{XBP}^{Ox}$	Yield coefficient of biomass on by-product under oxidation conditions [ $\text{kg kg}^{-1}$ ].
$K_{BP}$	Affinity constant of by-product [ $\text{kg m}^{-3}$ ].	$Y_{XG}^{Of}$	Yield coefficient of biomass on glucose under overflow conditions [ $\text{kg kg}^{-1}$ ].
$K_G$	Affinity constant of glucose [ $\text{kg m}^{-3}$ ].	$Y_{XG}^{Ox}$	Yield coefficient of biomass on glucose under oxidation conditions [ $\text{kg kg}^{-1}$ ].
$K_{IBP}^G$	Inhibition constant of by-product on glucose uptake [ $\text{kg m}^{-3}$ ].	$Y_{XO}^{BP}$	Yield coefficient of biomass on oxygen when growth is on by-product [ $\text{kg kg}^{-1}$ ].
$K_{IG}^G$	Inhibition constant of glucose on glucose uptake [ $\text{kg m}^{-3}$ ].	$Y_{XO}^G$	Yield coefficient of biomass on oxygen when growth is on glucose [ $\text{kg kg}^{-1}$ ].
$m_{BP}$	Maintenance coefficient for by-product [ $\text{kg kg}^{-1} \text{h}^{-1}$ ].	$\mu$	Specific growth rate [ $\text{h}^{-1}$ ].
$m_G$	Maintenance coefficient for glucose [ $\text{kg kg}^{-1} \text{h}^{-1}$ ].	$\mu_{BP}$	Specific growth rate on by-product [ $\text{h}^{-1}$ ].
$m_O$	Maintenance coefficient for oxygen [ $\text{kg kg}^{-1} \text{h}^{-1}$ ].	$\mu_{BP,max}$	Maximum specific growth rate on by-product [ $\text{h}^{-1}$ ].
$n$	Number of timesteps [-].	$\mu_{Comp}$	Specific growth rate in each compartment [ $\text{h}^{-1}$ ].
$O$	Dissolved oxygen concentration [ $\text{kg m}^{-3}$ ].	$\mu_{crit}$	Critical specific growth rate at which overflow metabolism starts [ $\text{h}^{-1}$ ].
$O^*$	Oxygen concentration at saturation [ $\text{kg m}^{-3}$ ].	$\mu_G$	Specific growth rate on glucose [ $\text{h}^{-1}$ ].
$OTR$	Oxygen transfer rate [ $\text{kg m}^{-3} \text{h}^{-1}$ ].	$\mu_{G,max}$	Maximum specific growth rate on glucose [ $\text{h}^{-1}$ ].
$q_{BP}$	Specific by-product uptake and formation rate [ $\text{kg kg}^{-1} \text{h}^{-1}$ ].		
$q_G$	Specific glucose uptake rate [ $\text{kg kg}^{-1} \text{h}^{-1}$ ].		
$q_{G,crit}$	Critical specific glucose uptake rate at which overflow		

simulation. Using this approach, it is possible to visualize the concentration of key components (e.g., glucose), something which is very challenging to do experimentally. This information can then be used to calculate key process metrics (e.g., the yield or productivity), thereby allowing different reactor configurations or operating conditions to be compared.

A related approach makes use of Lagrangian particle tracking. Here, particles representing the cells are introduced into the simulation domain and their progress is tracked as they move throughout the reactor [10]. From this it is possible to construct the history of the particle (often called its 'lifeline') [16]. Such an approach may be the most realistic representation of the processes occurring inside bioreactors, however, the tradeoff is the increased computational demand, and the need for more complex post-processing. Use of particle-tracking type approaches can provide statistical information about the conditions experienced by the microorganisms, for example the frequency at which they alternate between zones of high and low substrate concentration, as well as information about the length of these oscillations. This approach has been applied to a range of microorganisms, including *Clostridium ljungdahlii* [14], *Pseudomonas putida* [15], *Penicillium chrysogenum* [17] and *Saccharomyces cerevisiae* [9,12]. Both bubble column and stirred tank reactors have been examined, however little comparison between the two reactor types on the conditions experienced by the microorganisms has been provided in the open literature.

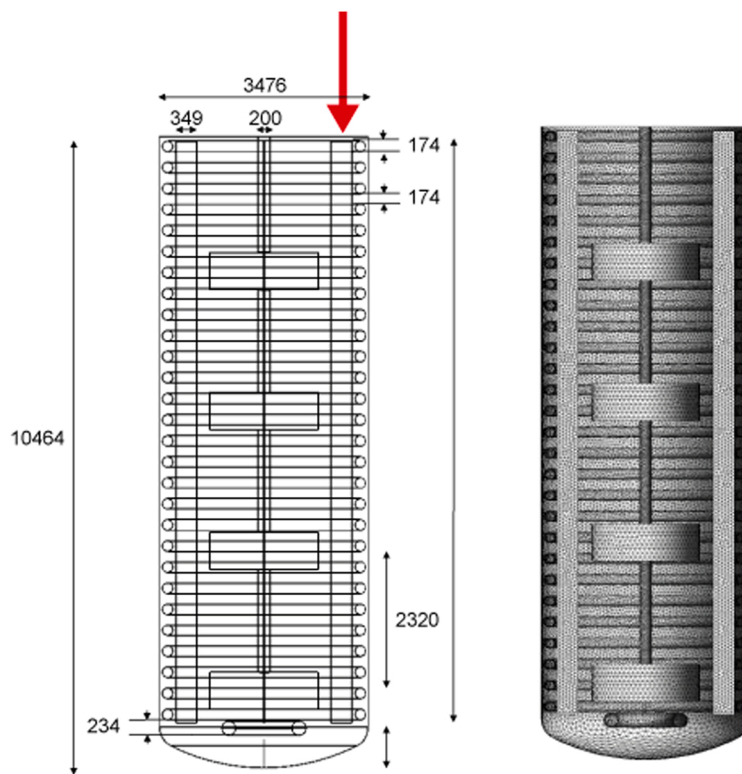
A major advantage of approaches based on Lagrangian particle tracking is that they may be the most meaningful from the perspective of understanding the conditions experienced by the cells as they move through the reactor. Another advantage of these type of approaches is that they provide information about the distribution of conditions experienced by the cells, unlike approaches based on the Eulerian framework which typically provide conditions averaged over the simulation volume and/or time. Exposure to heterogenous environmental conditions can drive population heterogeneity [18] which may have a negative effect on the overall process performance [19]. Hence there is a need to understand what conditions microorganisms are likely to experience in industrial bioreactors operated under representative

conditions. Similarly, detailed knowledge about the variety of conditions experienced in large-scale reactors is obviously useful in the design of scale-down systems [12]. Hence a key aim of this paper is to generate a dataset describing the conditions experienced in large-scale bioreactors for industrially representative microorganisms (i.e., *Escherichia coli* and *Saccharomyces cerevisiae*).

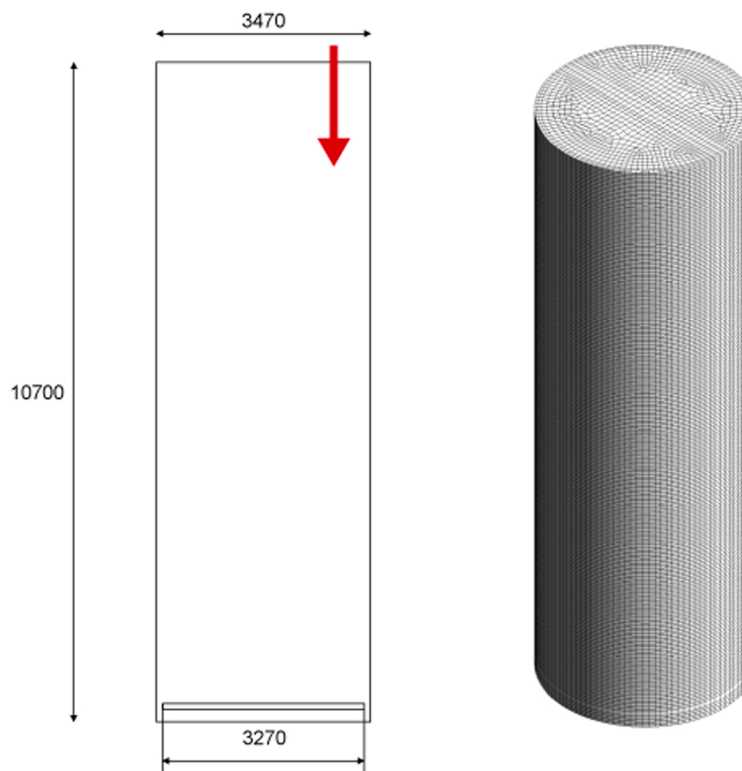
## 2. Methods

In this paper two industrially relevant configurations (a bubble column and a stirred tank with four six bladed Rushton impellers) have been investigated. Both configurations had a total volume of  $90 \text{ m}^3$ . This was selected as being broadly representative of large-scale bioreactors. The liquid volume was less in the bubble column reactor ( $64 \text{ m}^3$ ) than in the STR ( $73 \text{ m}^3$ ). This is due to the fact that the bubble column was operated at a higher gas volume fraction. These volumes were selected in order to represent an industrial fed-batch fermentation towards the end of the batch (i.e., when gradients are most likely to exist). In all cases the substrate was introduced at the top of the reactor. A schematic showing the two reactor configurations is given in Fig. 1.

Ansys CFX 19.2 was used to model the different reactor configurations. In all cases the Euler-Euler method was used to model the two-phase flow. All simulations were run in transient mode; unless stated otherwise reported results are transient averages. A single bubble size which was adjusted for the effect of static pressure was used in all simulations. This approach was used because the surface active compounds found in fermentation medium tend to favor a relatively narrow bubble size distribution [20]. Additionally, use of more complex models which account for a distribution of bubble sizes lead to substantially increased computational demand without marked increases in predictive performance [21]. Liquid-phase turbulence was modelled using the  $k-\epsilon$  model, while the dispersed-phase zero model was used to model gas phase turbulence. Simulations of the stirred tank configurations were performed using the transient rotor stator method where the time step was set to  $6 \times 10^{-3} \text{ s}$  to ensure that the impeller rotation was less than  $5^\circ$  per time step. A fixed time step of  $1 \times 10^{-3} \text{ s}$  was used for the bubble



Stirred tank



Bubble column

Fig. 1. Plot showing the different bioreactor configurations used in this work. Red arrows indicate the location where the feed was added, this point was located at a distance of 1.23 m from the centreline of the reactor, and a height of 9.9 m for the STR and 9 m for the bubble column.

column simulations. Detailed information about the meshes used, selection of inter-phase transfer models, boundary conditions and solution methods is presented elsewhere [22].

A total of 5000 particles were introduced to the system, these had a diameter of 1  $\mu\text{m}$  in order to mimic cells. These were introduced uniformly throughout the simulation domain. One-way coupling between the liquid and particle phases was used to reduce the computational demand. Such an approach is reasonable given the very small Stokes number of the particles. Particles were tracked for a total of 270 s for the bubble column and 150 s for the stirred tank.

In this work we have chosen to model two well characterized microorganisms with industrial applications, *Escherichia coli* and *Saccharomyces cerevisiae*. Scalars were introduced to the model to quantify the concentration of glucose, dissolved oxygen, ethanol and acetate. Source and sink terms were added to the scalar equation to account for consumption, production or addition of these components as appropriate.

In order to model the system, it is necessary to calculate the specific growth rate of the microorganism ( $\mu$ ), the specific rate of glucose uptake ( $q_G$ ), the specific rate of oxygen uptake ( $q_O$ ), as well as the rate at which the byproduct (ethanol or acetate) is produced or consumed ( $q_{BP}$ ). Here Monod kinetics have been used to calculate the specific growth rate. The specific growth rate varies depending on whether the substrate is glucose ( $\mu_G$ ) or the by-product ( $\mu_{BP}$ ). For *S. cerevisiae* the specific growth rate using glucose as the substrate is:

$$\mu_G = \frac{\mu_{G,\max} G}{K_G + G} \quad (1)$$

where  $\mu_{G,\max}$  is the maximum specific growth rate on glucose,  $G$  is the glucose concentration and  $K_G$  is the affinity constant for glucose. The effect of both substrate inhibition and by-product (acetate) inhibition were accounted for when calculating the growth rate of *E. coli* [23–25]:

$$\mu_G = \frac{\mu_{G,\max} G}{(K_G + G) \left(1 + \frac{BP}{K_{IBP}^G}\right)} \exp\left(-\frac{G}{K_{IG}^G}\right) \quad (2)$$

where  $K_{IBP}^G$  is the inhibition constant of by-product on glucose uptake and  $K_{IG}^G$  is the inhibition constant of glucose on glucose uptake. For both *S. cerevisiae* and *E. coli* the growth on by-product was modelled using:

$$\mu_{BP} = \frac{\mu_{BP,\max} BP}{K_{BP} + BP} \quad (3)$$

where  $\mu_{BP,\max}$  is the maximum specific growth rate where the by-product is used as the substrate,  $BP$  is the concentration of the byproduct and  $K_{BP}$  is the affinity constant for the by-product. Values used for these constants were obtained from the literature and are listed in Table 1.

In the approach used in this work five different metabolic regimes were considered, these being glucose starvation, oxidation, overflow, oxygen limitation and oxygen limitation and glucose starvation. The boundaries for these regimes depend on the physiology of the microorganism.

Glucose starvation occurs when the concentration of dissolved oxygen ( $O$ ) is sufficient to meet the maintenance requirements of the microorganism ( $m_O$ ), but the concentration of glucose ( $G$ ) is below that required to meet the maintenance requirements ( $m_G$ ). Expressed mathematically this is:

$$\frac{G}{t_s X} < m_G \quad \text{and} \quad \frac{O}{t_s X} > m_O \quad (4)$$

where  $X$  is the concentration of biomass and  $t_s$  is the timestep used in the simulation. Under these conditions it is assumed that any glucose in the medium is taken up, i.e.:

$$q_G = -\frac{G}{t_s X} \quad (5)$$

**Table 1** –

Values of parameters used in kinetic models. Parameters marked with an \* have been calculated based on information provided in the references.

Parameter	Units	<i>S. cerevisiae</i>		<i>E. coli</i>	
		Value	Reference	Value	Reference
$\mu_{BP,\max}$	$\text{h}^{-1}$	0.13	[27]	0.22	[28]
$\mu_{crit}$	$\text{h}^{-1}$	0.25	[27]	0.35	[29]
$\mu_{G,\max}$	$\text{h}^{-1}$	0.44	[27]	0.55	[23]
$K_{BP}$	$\text{kg m}^{-3}$	0.10	[30]	0.05	[28]
$K_G$	$\text{kg m}^{-3}$	0.15	[31]	0.05	[23]
$K_{IBP}^G$	$\text{kg m}^{-3}$	-		5	[23]
$K_{IG}^G$	$\text{kg m}^{-3}$	-		46.9	[24]
$m_{BP}$	$\text{kg kg}^{-1} \text{h}^{-1}$	0.01 *	[32]	0.04 *	[32,33]
$m_G$	$\text{kg kg}^{-1} \text{h}^{-1}$	0.02	[31]	0.04	[33]
$m_O$	$\text{kg kg}^{-1} \text{h}^{-1}$	0.02	[31]	0.01	[31]
$Y_{XBP}^{Of}$	$\text{kg kg}^{-1}$	0.11	90% of theoretical yield	0.22	[23]
$Y_{XBP}^{Ox}$	$\text{kg kg}^{-1}$	0.72	[30]	0.4	[23]
$Y_{XG}^{Of}$	$\text{kg kg}^{-1}$	0.05	[30]	0.15	[23]
$Y_{XG}^{Ox}$	$\text{kg kg}^{-1}$	0.49	[30]	0.51	[23]
$Y_{XO}^{BP}$	$\text{kg kg}^{-1}$	0.58 *	[32]	0.45 *	[31,32]
$Y_{XO}^G$	$\text{kg kg}^{-1}$	1.54 *	[32]	0.45	[31]

The specific byproduct uptake rate is:

$$q_{BP} = -\min\left(\frac{\mu_{BP}}{Y_{XBP}^{Ox}} + m_{BP}, \frac{BP}{t_s X}\right) \quad (6)$$

where  $m_{BP}$  is the maintenance requirement where the byproduct is used as a substrate and  $Y_{XBP}^{Ox}$  is the oxidative biomass yield on by-product. The specific oxygen uptake rate is:

$$q_O = -\min\left(\frac{\mu_G}{Y_{XO}^G} + \frac{\mu_{BP}}{Y_{XO}^{BP}} + m_O, \frac{\mu_{crit}}{Y_{XO}^G} + m_O\right) \quad (7)$$

where  $Y_{XO}^{BP}$  is the yield coefficient of biomass on oxygen where by-product is used as the substrate. In this regime growth only occurs due to by-product consumption:

$$\mu = \mu_{BP} \quad (8)$$

Oxygen limitation occurs when the concentration of dissolved oxygen is too low to meet maintenance requirements and the concentration of glucose is sufficient for maintenance:

$$\frac{G}{t_s X} > m_G \quad \text{and} \quad \frac{O}{t_s X} < m_O \quad (9)$$

Under these conditions the rate of glucose uptake is given by:

$$q_G = -\left(\frac{\mu_G}{Y_{XG}^{Of}} + m_G\right) \quad (10)$$

where  $Y_{XG}^{Of}$  is the yield coefficient of biomass on glucose under overflow conditions. When oxygen is limited by-product formation will occur, the specific rate being:

$$q_{BP} = \frac{\mu_G}{Y_{XBP}^{Of}} \quad (11)$$

where  $Y_{XBP}^{Of}$  is the yield of biomass on by-product under overflow conditions. Under oxygen limitation it is assumed that any dissolved oxygen is taken up to meet maintenance requirements, i.e.:

$$q_O = -\frac{O}{t_s X} \quad (12)$$

As the by-product can only be used under conditions where there is sufficient oxidative capacity the specific growth rate is:

$$\mu = \mu_G \quad (13)$$

Glucose starvation and oxygen limitation occur when the concentrations of both glucose and dissolved oxygen are insufficient to meet the maintenance requirements:

$$\frac{G}{t_s X} < m_G \quad \text{and} \quad \frac{O}{t_s X} < m_O \quad (14)$$

Here it is assumed that any glucose and dissolved oxygen present is consumed, meaning that Eq. (5) is used to determine the specific glucose uptake rate and Eq. (12) is used to determine the specific oxygen uptake rate. Under these conditions the specific growth rate and the rate of by-product consumption/uptake are both zero.

Oxidation occurs when the concentrations of both glucose and oxygen are sufficient to meet maintenance requirements, and the specific glucose uptake rate is less than the value ( $q_{G,crit}$ ) which will lead to overflow metabolism:

$$\frac{G}{t_s X} > m_G \quad , \quad \frac{O}{t_s X} > m_O \quad \text{and} \quad q_G < q_{G,crit} \quad (15)$$

The specific rate of glucose uptake is:

$$q_G = -\left(\frac{\mu_G}{Y_{XG}^{Ox}} + m_G\right) \quad (16)$$

where  $Y_{XG}^{Ox}$  is the yield coefficient of biomass on glucose under oxidative conditions. The rate of by-product consumption is given by:

$$q_{BP} = -\frac{\mu_{BP}}{Y_{XBP}^{Ox}} \quad (17)$$

where  $Y_{XBP}^{Ox}$  is the yield of biomass on by-product under oxidative conditions. Eq. (7) is used to determine the specific oxygen uptake rate. The specific growth rate is:

$$\mu = \mu_G + \mu_{BP} \quad (18)$$

Overflow conditions occur when the concentrations of dissolved oxygen and glucose are sufficient to meet maintenance requirements and the rate of glucose is above the critical value:

$$\frac{G}{t_s X} > m_G \quad , \quad \frac{O}{t_s X} > m_O \quad \text{and} \quad q_G > q_{G,crit} \quad (19)$$

The specific rate of glucose uptake is:

$$q_G = -\left(\frac{\mu_{crit}}{Y_{XG}^{Ox}} + \frac{\mu_G - \mu_{crit}}{Y_{XG}^{Of}} + m_G\right) \quad (20)$$

where  $\mu_{crit}$  is the specific growth rate that corresponds to the critical rate of glucose uptake. The rate of by-product production is:

$$q_{BP} = \frac{\mu_G - \mu_{crit}}{Y_{XBP}^{Of}} \quad (21)$$

Under overflow conditions Eq. (7) is used to determine the specific oxygen uptake rate, and the specific growth rate is determined using Eq. (13).

When modelling the STR using CFD the biomass concentration of

*E. coli* was  $133 \text{ kg m}^{-3}$ , while it was  $92.6 \text{ kg m}^{-3}$  for *S. cerevisiae*. Values for the bubble column were 102 and  $75.6 \text{ kg m}^{-3}$  for *E. coli* and *S. cerevisiae*, respectively. Given the relatively short time scale of the simulations it was assumed that the biomass concentrations were fixed. Glucose feed rates in the STR were  $674 \text{ kg h}^{-1}$  for *E. coli* and  $1030 \text{ kg h}^{-1}$  for *S. cerevisiae*, while values in the bubble column were  $327 \text{ kg h}^{-1}$  for *E. coli* and  $312 \text{ kg h}^{-1}$  for *S. cerevisiae*. Values of feed rates and biomass concentrations were obtained using a modelling approach described in our previous work [26]. In this approach it was assumed that the bioreactors were ideally mixed, and a PI controller was implemented with the aim of varying the feed rate such that the concentration of dissolved oxygen was 20% of saturation. Such an approach was used to mimic a common industrial strategy for the control of large-scale aerobic fermentations.

The bubble column was operated at a superficial velocity of  $0.16 \text{ m s}^{-1}$ , the STR was operated at a superficial velocity of  $0.07 \text{ m s}^{-1}$  and a stirring rate of 140 rpm. Volumetric power inputs were of the order  $1-2 \text{ kW m}^{-3}$  for the bubble column and  $5-6 \text{ kW m}^{-3}$  for the STR.

The particle tracks containing the particle time, location as well as the concentrations were exported to a text file. A custom script written in Matlab was used to process the file containing the particle data. As CFX uses a variable timestep for the particle integration the one-dimensional interpolation function (interp1) in Matlab was used to interpolate the results onto a regularly spaced ( $1 \times 10^{-4} \text{ s}$ ) vector using spline interpolation. This was done to simplify the subsequent calculations as performing the interpolation eliminates the need to account for different sampling times. Average values of the substrate and byproduct concentrations for each particle were calculated using the arithmetic mean. For example, the average glucose concentration ( $\bar{G}$ ) is defined as:

$$\bar{G} = \frac{1}{n} \sum_{i=1}^n G_i \quad (22)$$

where  $n$  is the number of time steps. The specific growth rate ( $\mu$ ) was calculated using the instantaneous glucose and byproduct concentrations using Eq. (1) for *S. cerevisiae* and Eq. (2) for *E. coli*. Results were then averaged over the particle time using the same approach as used for the substrate concentrations. The percentage of time spent by a particle in overflow conditions ( $F_O$ ) was found by:

$$F_O = \frac{\sum_{i=1}^n x_i}{n}, \quad x_i = \begin{cases} 1, & q_G > q_{G,crit} \\ 0, & q_G \leq q_{G,crit} \end{cases} \quad (23)$$

The fraction of time spent in starvation conditions ( $F_S$ ) was calculated in a similar fashion:

$$F_S = \frac{\sum_{i=1}^n x_i}{n}, \quad x_i = \begin{cases} 1, & \frac{G}{t_s X} < m_G \\ 0, & \frac{G}{t_s X} \geq m_G \end{cases} \quad (24)$$

The length of each fluctuation was also determined using the particle track data.

### 3. Results

Plots showing the transient average glucose, acetate/ethanol and dissolved oxygen concentrations for the two reactor configurations are shown in Fig. 2 for *E. coli* and in Fig. 3 for *S. cerevisiae*. It was found that there was a 'hotspot' of high glucose concentration near the feed-point, this occurred for both reactor configurations and microorganisms examined. As discussed in our previous work [22] the hydrodynamics in the STR gives rise to higher mixing times (approximately 200 s, compared with  $\sim 30 \text{ s}$  for the bubble column). This is apparent when examining the concentrations of ethanol and dissolved oxygen, with the STR having more pronounced axial gradients. Such results are unsurprising, as the use of multiple radial impellers (e.g. Rushton turbines) is

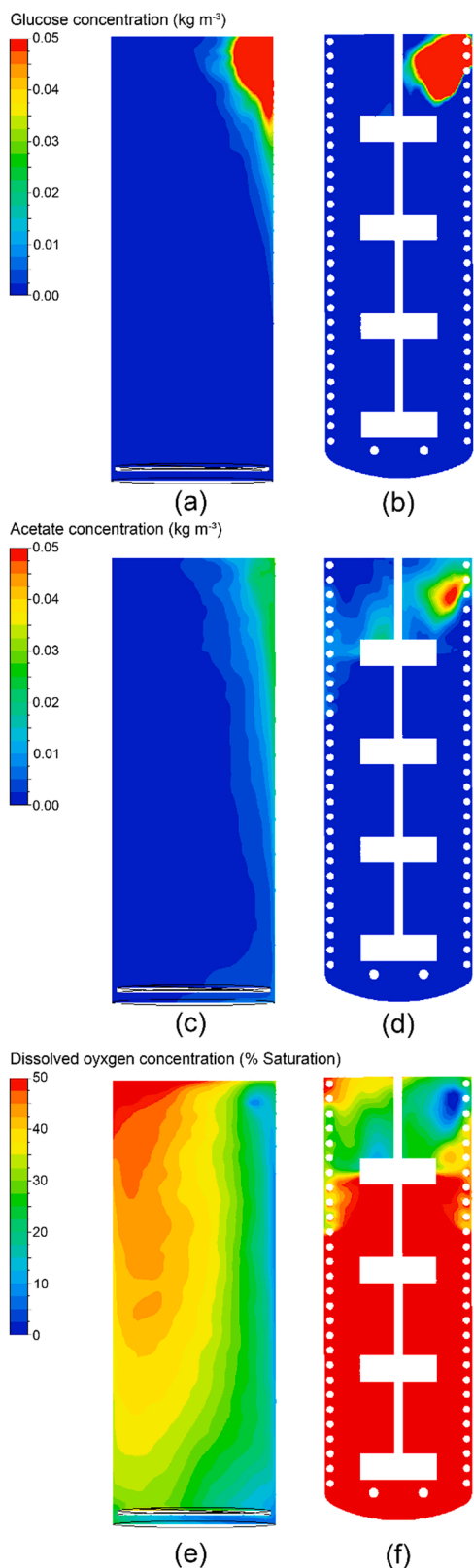


**Fig. 2.** – Plot showing the transient average concentrations of glucose (a-b), acetate (c-d) and dissolved oxygen (e-f) for growth of *E. coli*. Results in the first column (i.e. (a), (c) and (e)) are for the bubble column, while those in the second column (i.e. (b), (d) and (f)) are for the STR. Results for the STR have only been shown for the tank domain.

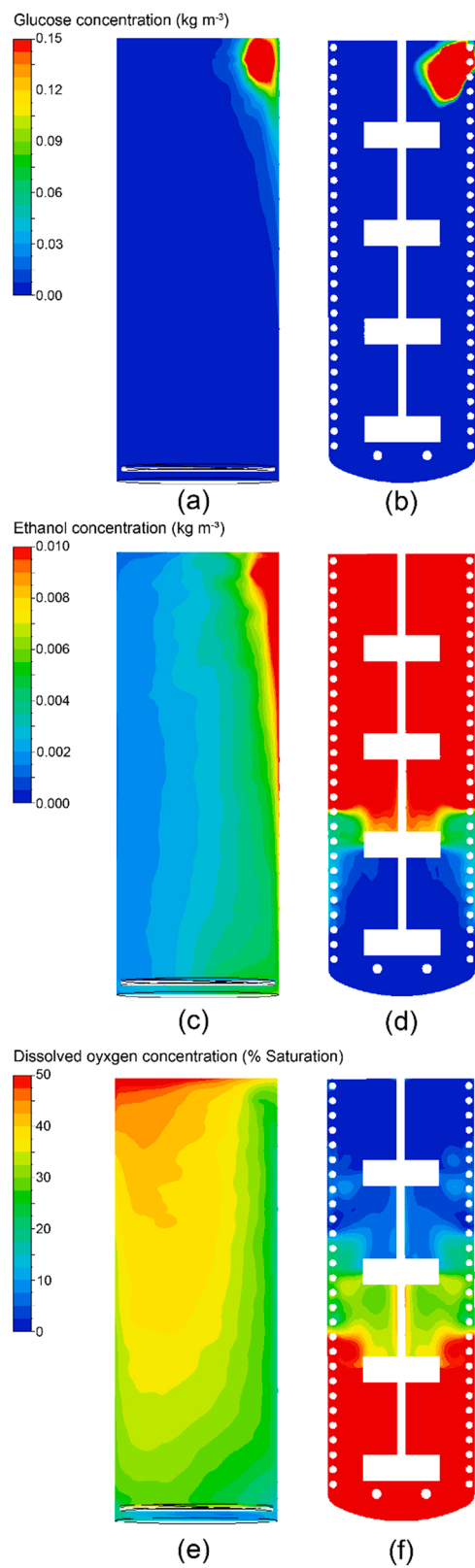


**Fig. 3.** Plot showing the transient average concentrations of glucose (a-b), ethanol (c-d) and dissolved oxygen (e-f) for growth of *S. cerevisiae*. Results in the first column (i.e. (a), (c) and (e)) are for the bubble column, while those in the second column (i.e. (b), (d) and (f)) are for the STR. Results for the STR have only been shown for the tank domain.

likely to lead to a degree of compartmentalization. Here it must also be noted that our previous work examined mixing in a system with three axial flow (A310) and one radial impeller; mixing in this case was slightly better than the case with four Rushton impellers, but still not as good as the bubble column [22].

As would be expected the differences in mixing behaviour give rise to different metabolic regimes experienced by the microorganisms, and this is shown in Fig. 4. It was found in all cases that the zone of high substrate concentration at the feed point led to a volume of the reactor where overflow metabolism occurred, and that this zone was larger by a factor of 3–6 for the stirred tank cases. Another major difference between the reactor configurations was the volume experiencing glucose starvation, this was between 6% and 50% for the bubble column and

approximately 90% for the stirred tank reactor. These results suggest that the glucose introduced into the reactor is being consumed in the zone near the top impeller (see Fig. 2 and Fig. 3) before it can be mixed throughout the vessel. In the case of the bubble column the glucose is transported more evenly throughout the reactor, which reduces the volume experiencing starvation. Interestingly, a large difference between the organisms was observed for the bubble column case (as shown in Fig. 4). This may be due to the fact that the maintenance requirements for *E. coli* are double that of *S. cerevisiae*, meaning that it is much more likely that the glucose starvation regime will be experienced.

Knowledge of the metabolic regimes experienced within the reactor is obviously relevant to key process parameters. For example, in the production of baker's yeast a key objective is maximising the biomass yield on substrate. To achieve this objective, it is important to avoid overflow metabolism, as this leads to ethanol production and hence a reduction in the overall yield. Using the CFD model it is possible to determine the proportion of feed which is diverted to overflow metabolism, this was 12% of the glucose added for the STR case and 3% for the bubble column (percentages have been calculated on a mass basis). Understanding how the feedstock is converted to different products or metabolites is key in quantifying the overall process performance. This is more complex in the case of *E. coli* which is often used to produce recombinant proteins. The availability of substrate within the reactor will clearly affect the ability of the cell to correctly synthesise the desired protein product, however, this relationship is more complex than the production of biomass, as it is necessary to account for the synthesis of the recombinant protein in addition to the normal cellular processes. Process performance in this case can be complicated by other factors (e.g. the choice of expression system, the protein being produced and its metabolic burden, etc.) [19].

It is also possible to quantify the performance of the bioreactors using particle tracking methods. These give an insight into the conditions experienced by the cells as they travel throughout the reactor and hence may offer the most representative methodology of quantifying reactor performance. Fig. 5 shows a plot of the average glucose concentrations experienced by the particles for the reactor configurations examined. It was found that on average most of the particles experienced low glucose concentrations, this being in line with the results shown in Figs. 2–4. Using the kinetic model, it is possible to calculate the glucose concentration which will lead to the organism growing at the critical growth rate, this is  $0.0875 \text{ kg m}^{-3}$  for *E. coli* (neglecting substrate and acetate inhibition) and  $0.197 \text{ kg m}^{-3}$  for *S. cerevisiae*. As shown in Fig. 5 the average conditions experienced by the microorganisms in the reactor are typically below this value (except for a small fraction of the *E. coli* population). It is also possible to generate similar plots for the dissolved oxygen concentration, however these results have not been shown as oxygen limitation was not found to be significant in the cases examined. This is because the values of the cell density and glucose feed rate were obtained from a model where the control objective was to maintain a fixed level of dissolved oxygen (20% of saturation), meaning oxygen limitation is unlikely to occur. An obvious interesting avenue for future work would be to explore the performance if alternative control strategies are used (e.g., if the aim is to maximise the biomass productivity).

Data about the glucose concentrations found in the bioreactor can also be used to calculate the metabolic regimes experienced by the microorganisms. Results are shown in Fig. 6 for overflow and in Fig. 7 for starvation. Results from Fig. 6 show that approximately 1% of the particles spend more than 10% of the time in overflow conditions. This is unsurprising given the fluid flow patterns found in the reactor, where particles are likely to move quickly through the zone of high substrate concentration near the feed. This behaviour was similar for both reactor configurations and microorganisms examined. A major difference between the reactor configurations was found when analysing the fraction of time the particles spent in starvation conditions (Fig. 7). It was observed that the population distribution in the STRs was essentially bimodal, with approximately 40% of the population not experiencing

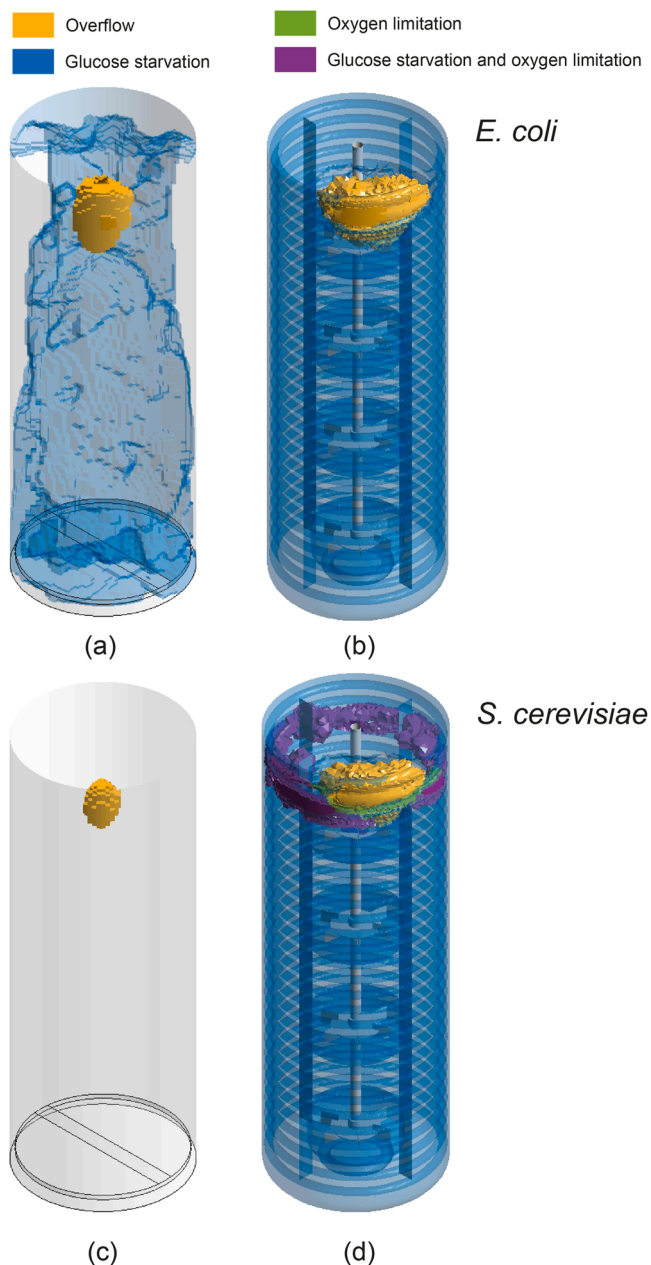
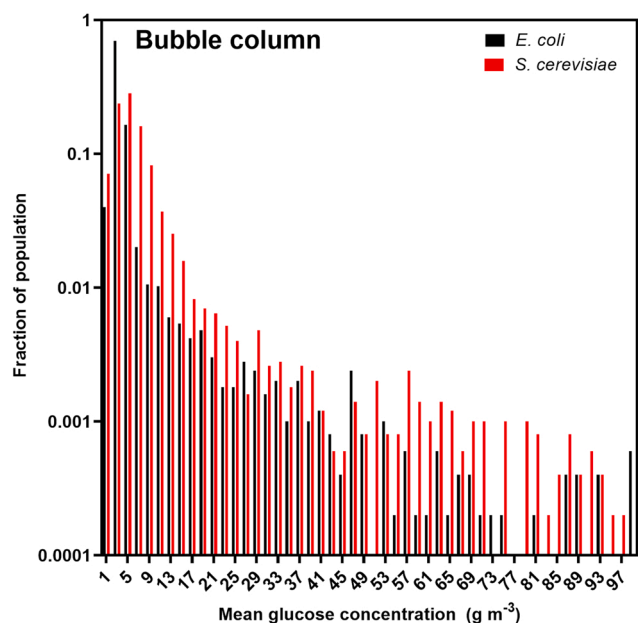
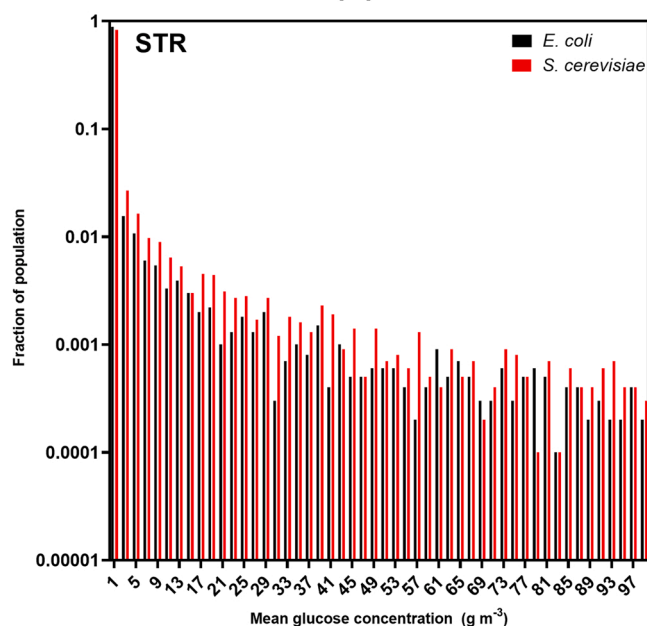


Fig. 4. Plot showing the different metabolic regimes experienced in the bubble column bioreactors (a) and (c) and in the STRs (b) and (d). Results in the first row (a-b) are for *E. coli*, results in the second row (c-d) are for *S. cerevisiae*. The oxidation regime has not been coloured, if the reactor volume is not in one of the other four metabolic regimes then it is in oxidative metabolism. Results for the bubble columns have been clipped at the gas-liquid interface.



(a)



(b)

Fig. 5. Plot showing the average glucose concentrations calculated based on the particle tracks. Results are shown for the bubble column (a) and the STR (b). Note the logarithmic scale on the y-axis.

starvation to a significant extent, with the remaining 60% of the population spending a relatively large (> 70%) fraction of time exposed to starvation conditions. In contrast, 90% of the population of particles in the bubble column spent less than a third of the time exposed to starvation conditions. The differences between the two reactor configurations are most likely explained by the differences in mixing behaviour; as previously discussed the flow in the STR is much more stratified, meaning that it is more likely for the particles to be ‘trapped’ in a zone of low substrate concentration. Exposure to starvation conditions for a significant length of time is likely to trigger a stress response in the microorganisms and this will have an impact on the process performance.

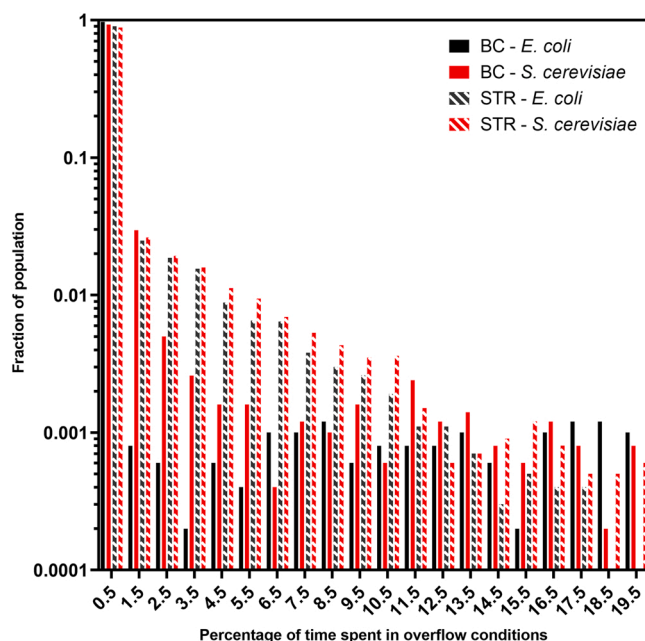


Fig. 6. Plot showing the percentage of time spent in overflow conditions for the bubble column and STR. Note the logarithmic scale on the y-axis.

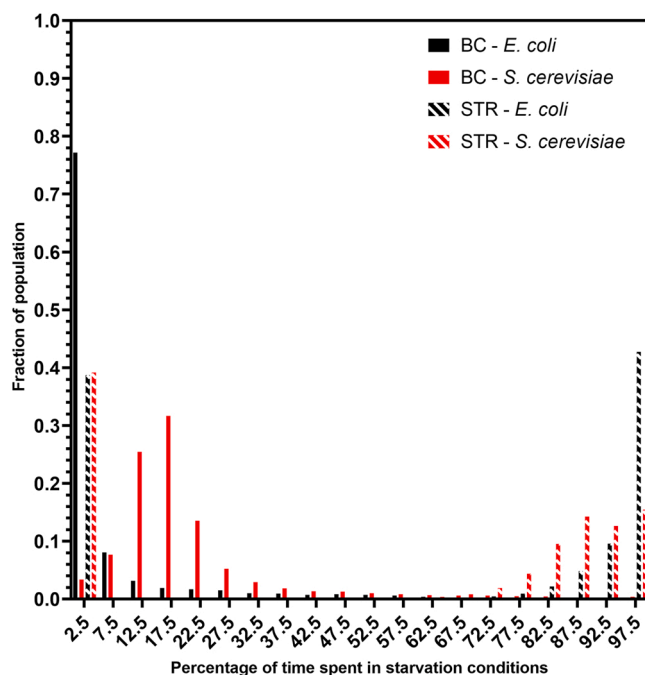


Fig. 7. Plot showing the percentage of time each particle spends in starvation conditions for the bubble column and STR configurations examined.

Fig. 8 shows the distribution of the average specific growth rates calculated for the cases examined. Unsurprisingly for the STRs it was found that the majority cells are growing at a relatively small fraction of the maximum value; 98% of the *S. cerevisiae* cells and 99% of the *E. coli* cells were determined to be growing at or less than 7.5% of the maximum rate. Specific growth rates were found to be higher in the bubble column, this again is most likely due to the more homogenous distribution of substrate due to differences in mixing behaviour.

An advantage of using the particle tracking approach is that it is possible to quantify the length of the fluctuations. Cumulative distributions showing the fraction of the total fluctuations as a function of the

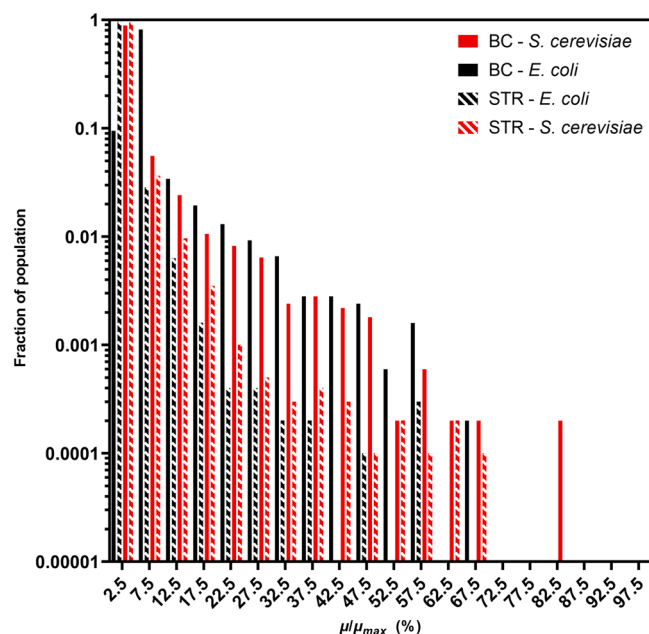


Fig. 8. Plot showing the distribution of average specific growth rates calculated for the particle populations in the two bioreactor configurations examined. To enable comparison the growth rates have been normalised as a fraction of the maximum; note the logarithmic y-axis.

length are plotted for overflow conditions in Fig. 9 and starvation conditions in Fig. 10. Once again differences between the reactor designs are apparent, with the fluctuations in the bubble column tending to be smaller in duration. For example, 99% of the fluctuations (i.e., exposure to starvation or overflow conditions) in the bubble column are predicted to be 2 s or less in duration. This contrasts with the STR where a larger fraction of the particles is exposed to longer duration fluctuations.

A key consideration in analysing the results shown in Fig. 9 and Fig. 10 is understanding what duration of fluctuations are likely to lead to a response from the cells. For example, a large fraction of the fluctuations in the bubble column are less than 0.1 s in length; such short

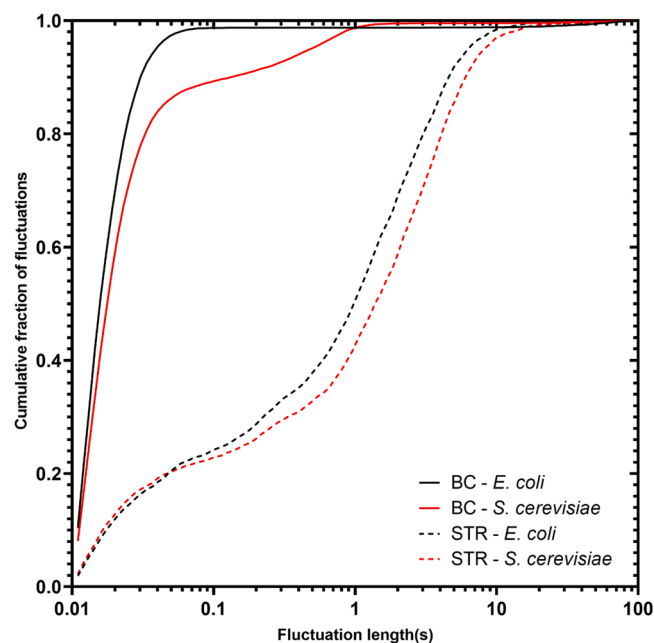


Fig. 9. Plot showing the cumulative fraction of fluctuations as a function of the fluctuation length for overflow conditions.

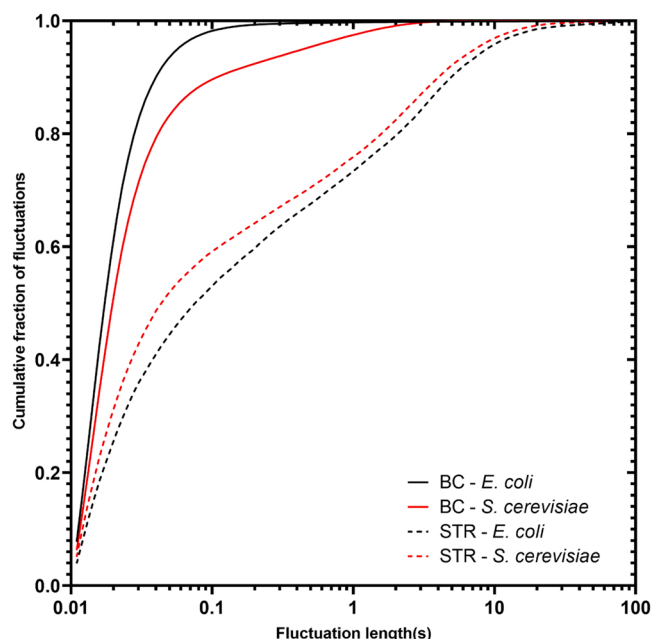


Fig. 10. Plot showing the cumulative fraction of all fluctuations as a function of their length for starvation conditions.

exposures to changing conditions may not lead to any changes in cellular physiology. Contrastingly, as the length of the fluctuation increases (i.e., cells are exposed to starvation or overflow conditions for a longer time) it is more likely that they will respond to this in some way. It has been shown [34] that *E. coli* is able to rapidly (< 100 s) modulate its metabolism in response to environmental changes, and that exposure to glucose starvation for periods of 30–70 s leads to changes in the metabolome [35]. On this basis it would be reasonable to think that the conditions found in the STRs are likely to lead to a physiological change for at least some part of the population. Such conditions can impose a significant metabolic burden on the cells (reported to be a 40–50% increase in ATP maintenance demands), as they involve large changes in gene regulation [35]. This can lead to an increase in the maintenance requirement for cells exposed to fluctuating conditions; it has also been shown that deletion of selected genes can both reduce the maintenance requirements and increase the yield of the product [36].

When examining these results, it is important to note that they depend on the selection of suitable metabolic models, and that the choice of model will have a significant impact upon the results. It is also important to note that the values used to determine whether or not starvation or overflow metabolism occurs are not likely to be fixed, as was the case in this manuscript. Microorganisms are capable of regulating the uptake rate of nutrients based on their concentration in the environment [37]. Hence, the values of key constants (e.g.,  $K_G$ ,  $m_G$ ) will change based on the history of the cell, and there may exist a distribution of cells with different adaptations to the environment. An area for future work could be to explore the effect of this on the predicted extent of starvation and overflow within the reactor. One way in which this could be done is to make the current uptake rates a function of both the local concentrations as well as the history of the particle. This would involve having a detailed biological understanding of how the history of a cell affects its current and future behaviour, as well as developing computational tools by which this can be implemented.

In designing a scale-down system it is important to know what conditions the cells will be exposed to, as well as the amount of time they will be exposed to these conditions. This information can then be used to determine the residence time in vessels (e.g. in two-tank set-ups) [38,39] or the oscillating feed supply in other systems [40]. Such information can be obtained from the particle track data. The length of both

starvation and overflow fluctuations was discretised into one second intervals, and the number of each of these oscillations has been plotted in Fig. 11 for overflow and in Fig. 12 for starvation. The dataset used to generate these figures is provided in the Supplementary Material. These data can be combined with the information shown in Fig. 6 and Fig. 7 to generate industrially representative data for scale-down systems.

#### 4. Conclusions

In this work CFD models of large-scale bubble columns and stirred tank bioreactors were combined with the growth kinetics for *E. coli* and *S. cerevisiae*, two widely used microorganisms in industrial biotechnology. The effect of the reactor design on the process performance was quantified using volume-averaged data from the CFD, as well as using a Lagrangian particle tracking approach, where cells are tracked as they move through the vessel. It was found that the bubble column generally offered better performance, and this is thought to be due to its improved mixing characteristics when compared with the STR.

Use of the Lagrangian particle tracking approach can provide detailed information about the conditions experienced by the cells in the reactor. For example, it is possible to quantify the duration and frequency of any fluctuations in conditions. Such data can then be used in the construction of representative scale-down systems. This work provides a detailed dataset for industrially representative reactor configurations which can be used for this goal.

#### Declaration of Competing Interest

The authors declare the following financial interests/personal relationships which may be considered as potential competing interests: Gisela Nadal-Rey reports financial support and equipment, drugs, or supplies were provided by Novozymes. Gisela Nadal-Rey, Benny Cassels, Sjeff Cornelissen reports a relationship with Novozymes that includes: employment. Authors of this paper have been or are employees of Novozymes A/S. (GNR, BC and SC).

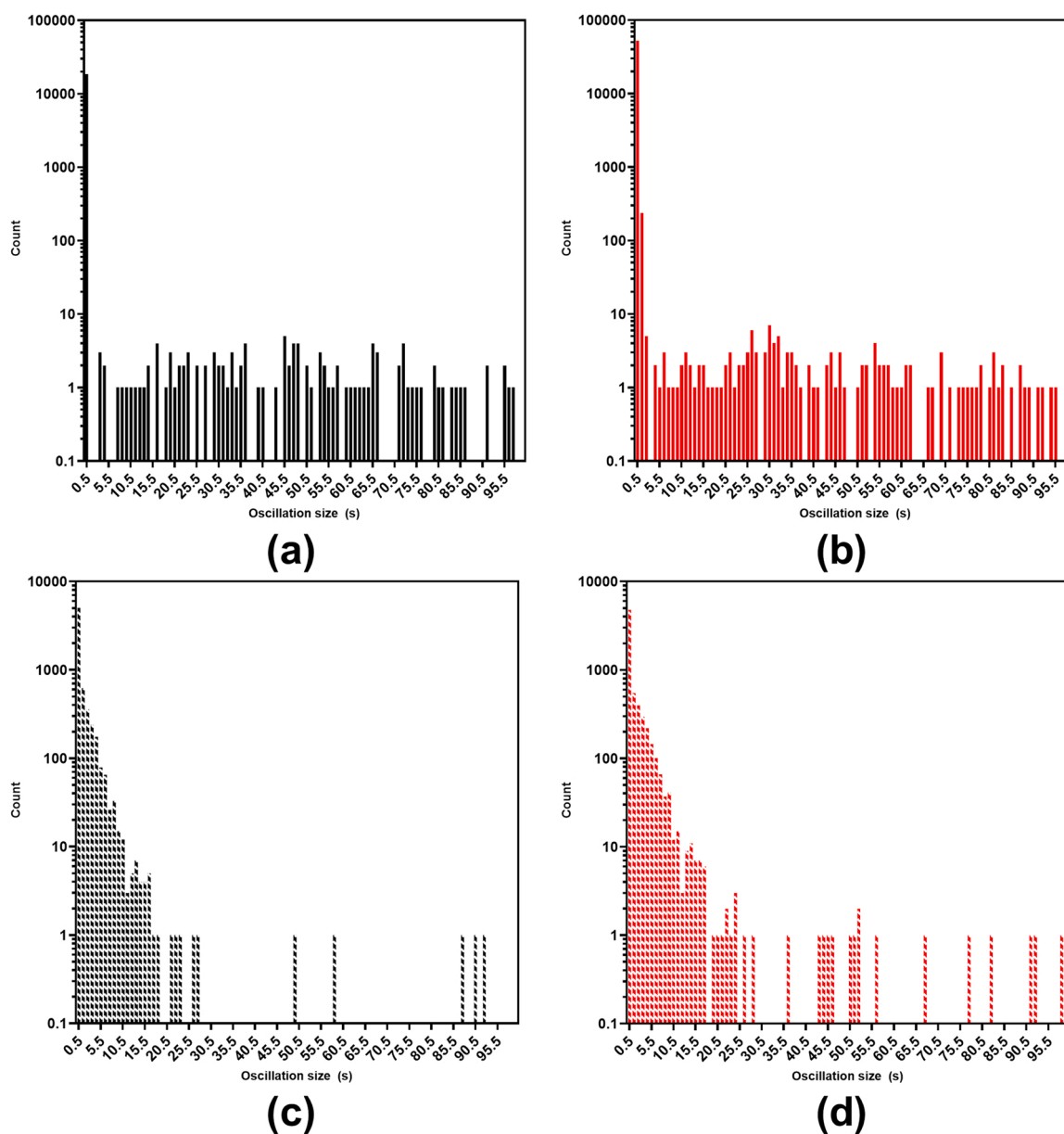


**Fig. 11.** Plot showing the number of overflow fluctuations for the different microorganisms and reactor configurations examined. Results are shown for the bubble column with *E. coli* (a), the bubble column with *S. cerevisiae* (b), the STR with *E. coli* (c) and the STR with *S. cerevisiae* (d).

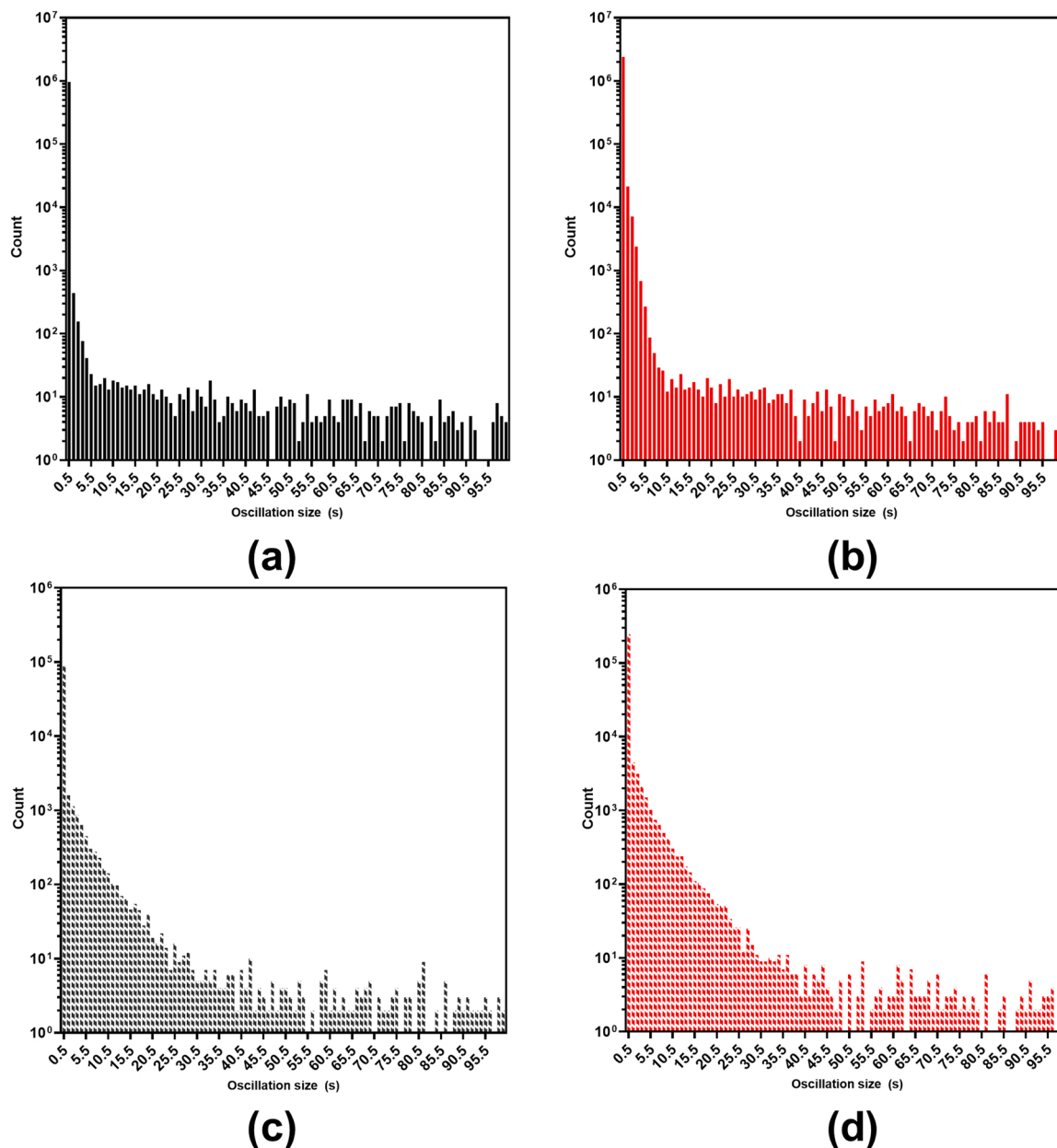


Fig. 12. Plot showing the number of starvation fluctuations for the different microorganisms and reactor configurations examined. Results are shown for the bubble column with *E. coli* (a), the bubble column with *S. cerevisiae* (b), the STR with *E. coli* (c) and the STR with *S. cerevisiae* (d).

### Data Availability

Data have been made available in a repository, details are in the data availability statement.

### Acknowledgements

This work was supported by the Technical University of Denmark and Novozymes A/S. The authors acknowledge the DTU Computing Centre, the Sydney Informatics Hub and the University of Sydney's high-performance computing cluster, Artemis, for providing the computing resources that have contributed to the results reported herein.

### Appendix A. Supporting information

Supplementary data associated with this article can be found in the online version at [doi:10.1016/j.bej.2023.108989](https://doi.org/10.1016/j.bej.2023.108989).

### References

- [1] G. Larsson, M. Törnkvist, E.S. Wernersson, C. Trägårdh, H. Noorman, S.O. Enfors, Substrate gradients in bioreactors: origin and consequences, *Bioprocess Biosyst. Eng.* 14 (1996) 281–289.
- [2] G. Nadal-Rey, D.D. McClure, J.M. Kavanagh, S. Cornelissen, D.F. Fletcher, K. V. Gernaey, Understanding gradients in industrial bioreactors, *Biotechnol. Adv.* 46 (2021), 107660.
- [3] J.S. Crater, J.C. Lievens, Scale-up of industrial microbial processes, *FEMS microbiology letters*, 365 (2018) fny138.
- [4] A.J.J. Straathof, S.A. Wahl, K.R. Benjamin, R. Takors, N. Wierckx, H.J. Noorman, Grand Research Challenges for Sustainable Industrial Biotechnology, *Trends Biotechnol.* 37 (2019) 1042–1050.
- [5] P.M. Doran, *Bioprocess Engineering Principles and Technology*, Elsevier Science, Waltham, MA, 2012.
- [6] S.O. Enfors, M. Jahic, A. Rozkov, B. Xu, M. Hecker, B. Jürgen, E. Krüger, T. Schweder, G. Hamer, D. O'Beirne, N. Noisommit-Rizzi, M. Reuss, L. Boone, C. Hewitt, C. McFarlane, A. Nienow, T. Kovacs, C. Trägårdh, L. Fuchs, J. Revstedt, P.C. Friberg, B. Hjertager, G. Blomsten, H. Skogman, S. Hjort, F. Hoeks, H.Y. Lin, P. Neubauer, R. van der Lans, K. Luyben, P. Vrabel, Å. Manelius, Physiological responses to mixing in large scale bioreactors, *J. Biotechnol.* 85 (2001) 175–185.

- [7] S. George, G. Larsson, K. Olsson, S.O. Enfors, Comparison of the Baker's yeast process performance in laboratory and production scale, *Bioprocess Biosyst. Eng.* 18 (1998) 135–142.
- [8] F. Bylund, E. Collet, S.O. Enfors, G. Larsson, Substrate gradient formation in the large-scale bioreactor lowers cell yield and increases by-product formation, *Bioprocess Eng.* 18 (1998) 171–180.
- [9] D.D. McClure, J.M. Kavanagh, D.F. Fletcher, G.W. Barton, Characterizing bubble column bioreactor performance using computational fluid dynamics, *Chem. Eng. Sci.* 144 (2016) 58–74.
- [10] A. Lapin, J. Schmid, M. Reuss, Modeling the dynamics of *E. coli* populations in the three-dimensional turbulent field of a stirred-tank bioreactor—a structured-segregated approach, *Chem. Eng. Sci.* 61 (2006) 4783–4797.
- [11] G. Wang, C. Haringa, W. Tang, H. Noorman, J. Chu, Y. Zhuang, S. Zhang, Coupled metabolic-hydrodynamic modeling enabling rational scale-up of industrial bioprocesses, *Biotechnol. Bioeng.* 117 (2020) 844–867.
- [12] C. Haringa, A.T. Deshmukh, R.F. Mudde, H.J. Noorman, Euler-Lagrange analysis towards representative down-scaling of a 22 m<sup>3</sup> aerobic *S. cerevisiae* fermentation, *Chem. Eng. Sci.* 170 (2017) 653–669.
- [13] J. Morchain, J.-C. Gabelle, A. Cockx, A coupled population balance model and CFD approach for the simulation of mixing issues in lab-scale and industrial bioreactors, *AIChE J.* 60 (2014) 27–40.
- [14] F. Siebler, A. Lapin, M. Hermann, R. Takors, The impact of CO gradients on C. ljungdahlii in a 125 m<sup>3</sup> bubble column: Mass transfer, circulation time and lifeline analysis, *Chem. Eng. Sci.* 207 (2019) 410–423.
- [15] M. Kuschel, F. Siebler, R. Takors, Lagrangian trajectories to predict the formation of population heterogeneity in large-scale bioreactors, *Bioengineering* 4 (2017) 27.
- [16] L. Blöbaum, C. Haringa, A. Grünberger, Microbial lifelines in bioprocesses: from concept to application, *Biotechnol. Adv.* (2022), 108071.
- [17] C. Haringa, W. Tang, A.T. Deshmukh, J. Xia, M. Reuss, J.J. Heijnen, R.F. Mudde, H. J. Noorman, Euler-Lagrange computational fluid dynamics for (bio)reactor scale down: an analysis of organism lifelines, *Eng. Life Sci.* 16 (2016) 652–663.
- [18] A.-L. Heins, D. Weuster-Botz, Population heterogeneity in microbial bioprocesses: origin, analysis, mechanisms, and future perspectives, *Bioprocess Biosyst. Eng.* 41 (2018) 889–916.
- [19] P. Rugbjerg, N. Myling-Petersen, A. Porse, K. Sarup-Lytzen, M.O.A. Sommer, Diverse genetic error modes constrain large-scale bio-based production, *Nat. Commun.* 9 (2018) 787.
- [20] D.D. McClure, J.M. Kavanagh, D.F. Fletcher, G.W. Barton, Development of a CFD model of bubble column bioreactors: part one – a detailed experimental study, *Chem. Eng. Technol.* 36 (2013) 2065–2070.
- [21] Z. Huang, D.D. McClure, G.W. Barton, D.F. Fletcher, J.M. Kavanagh, Assessment of the impact of bubble size modelling in CFD simulations of alternative bubble column configurations operating in the heterogeneous regime, *Chem. Eng. Sci.* 186 (2018) 88–101.
- [22] G. Nadal-Rey, D.D. McClure, J.M. Kavanagh, B. Cassells, S. Cornelissen, D. F. Fletcher, K.V. Gernaey, Computational fluid dynamics modelling of hydrodynamics, mixing and oxygen transfer in industrial bioreactors with Newtonian broths, *Biochem. Eng. J.* 177 (2022), 108265.
- [23] B. Xu, M. Jahic, S.-O. Enfors, Modeling of overflow metabolism in batch and fed-batch cultures of *Escherichia coli*, *Biotechnol. Prog.* 15 (1999) 81–90.
- [24] J. Ruiz, G. González, C. de Mas, J. López-Santín, A semiempirical model to control the production of a recombinant aldolase in high cell density cultures of *Escherichia coli*, *Biochem. Eng. J.* 55 (2011) 82–91.
- [25] K. Han, O. Levenspiel, Extended monod kinetics for substrate, product, and cell inhibition, *Biotechnol. Bioeng.* 32 (1988) 430–447.
- [26] G. Nadal-Rey, D.D. McClure, J.M. Kavanagh, B. Cassells, S. Cornelissen, D. F. Fletcher, K.V. Gernaey, Development of dynamic compartment models for industrial aerobic fed-batch fermentation processes, *Chem. Eng. J.* 420 (2021), 130402.
- [27] T. Paalme, R. Elken, R. Vilu, M. Korhola, Growth efficiency of *Saccharomyces cerevisiae* on glucose/ethanol media with a smooth change in the dilution rate (A-stat), *Enzym. Microb. Technol.* 20 (1997) 174–181.
- [28] T. Paalme, R. Elken, A. Kahru, K. Vanatalu, R. Vilu, The growth rate control in *Escherichia coli* at near to maximum growth rates: the A-stat approach, *Antonie Van Leeuwenhoek* 71 (1997) 217–230.
- [29] T. Paalme, K. Tiisma, A. Kahru, K. Vanatalu, R. Vilu, Glucose-limited fed-batch cultivation of *Escherichia coli* with computer-controlled fixed growth rate, *Biotechnol. Bioeng.* 35 (1990) 312–319.
- [30] B. Sonnleitner, O. Käppli, Growth of *Saccharomyces cerevisiae* is controlled by its limited respiratory capacity: Formulation and verification of a hypothesis, *Biotechnol. Bioeng.* 28 (1986) 927–937.
- [31] J. Villadsen, J.H. Nielsen, G. Lidén, *Bioreaction Engineering Principles*, 3rd ed., Springer US, Boston, MA, 2011.
- [32] J.J. Heijnen, J.A. Roels, A macroscopic model describing yield and maintenance relationships in aerobic fermentation processes, *Biotechnol. Bioeng.* 23 (1981) 739–763.
- [33] L. Andersson, L. Strandberg, L. Haggström, S.-O. Enfors, Modeling of high cell density fed batch cultivation, *FEMS Microbiol. Rev.* 14 (1994) 39–44.
- [34] S. Sunya, F. Delvigne, J.-L. Uribelarrea, C. Molina-Jouve, N. Gorret, Comparison of the transient responses of *Escherichia coli* to a glucose pulse of various intensities, *Appl. Microbiol. Biotechnol.* 95 (2012) 1021–1034.
- [35] M. Löffler, J.D. Simen, G. Jäger, K. Schäferhoff, A. Freund, R. Takors, Engineering *E. coli* for large-scale production – Strategies considering ATP expenses and transcriptional responses, *Metab. Eng.* 38 (2016) 73–85.
- [36] M. Ziegler, J. Zieringer, C.-L. Döring, L. Paul, C. Schaal, R. Takors, Engineering of a robust *Escherichia coli* chassis and exploitation for large-scale production processes, *Metab. Eng.* 67 (2021) 75–87.
- [37] E. Postma, W. Alexander Scheffers, J.P. Van Dijken, Kinetics of growth and glucose transport in glucose-limited chemostat cultures of *Saccharomyces cerevisiae* CBS 8066, *Yeast* 5 (1989) 159–165.
- [38] A.R. Lara, E. Galindo, R.T. Octavio, L.A. Palomares, Living with heterogeneities in bioreactors: Understanding the effects of environmental gradients on cells, *Mol. Biotechnol.* 34 (2006) 355.
- [39] P. Neubauer, S. Junne, Scale-up and scale-down methodologies for bioreactors, *Bioreactors* (2016) 323–354.
- [40] P. Ho, S. Täuber, B. Stute, A. Grünberger, E. von Lieres, Microfluidic reproduction of dynamic bioreactor environment based on computational lifelines, *Front. Chem. Eng.* 4 (2022), 826485.